Towards a quantitative indicator of feather disruption following the cleansing of oiled birds

Towards a quantitative indicator of feather disruption following the cleansing of oiled birds

Stephen W. Bigger[1*], Lawrence N. Ngeh[1], Peter Dann[2] and John D. Orbell[1]

1. Institute for Sustainability and Innovation, College of Engineering and Science, Victoria University, PO Box 14428, Melbourne, 8001, Australia.
2. Research Department, Phillip Island Nature Parks, PO Box 97, Cowes, Phillip Island, 3991, Australia.

REVISED MANUSCRIPT

Abstract

A computer-based imaging method for determining feather microstructure coherency following a cleansing treatment, was developed, calibrated and trialled on Mallard Duck (*Anas platyrhyhchos*) feathers. The feathers were initially contaminated with a light crude oil and then cleansed by either detergent (Deacon 90) treatment or, alternatively, by magnetic particle technology (MPT) using iron powder. The imaging method provides a single quantitative parameter for the coherence of feather microstructure and the results confirm that MPT treatment imparts less disruption to the feather microstructure than detergent treatment. It is proposed that this imaging method can be developed and implemented for the assessment of feather disruption and possibly damage, either for the trialling of different treatment protocols, or as a tool during the rehabilitation process, along with other such indicators, to give a more comprehensive assessment of feather condition than is currently available.

Key Words

Computer-imaging; feather microstructure coherency; magnetic particle cleansing; oil-soaked birds

Highlights

- Computer-based imaging method developed to quantitatively assess feather coherency.
- Imaging method successfully applied in studying cleansing of oil-soaked feathers and to feather coherency assessment.
- Cleansing feathers magnetically imparts less disruption to feather integrity than detergent methods.

*Author for correspondence

1. Introduction

Magnetic particle technology (MPT) has demonstrated great utility in a range of discipline areas (Safarikova & Safarik, 2001) and is a convenient and quick means by which oil-soaked wildlife can be cleansed (Orbell *et al*., 2007). This innovative approach has been investigated and developed for the clean-up of oil-soaked species such as the Mallard Duck (*Anas platyrhynchos*) and Little Penguin (*Eudyptula minor*) (Orbell *et al*., 2004). This technology has the advantage of being portable and enables oil to be removed immediately in the field, upon first encounter, either directly or with the aid of pre-treatment agents in cases where the oil residues are highly weathered and/or persistent (Ngeh *et al*., 2012).

Two further advantages of MPT technology over detergent-based techniques for oil removal are its high efficiency and its purported ability to invoke less damage to the feather microstructure (Orbell *et al*., 2007). In relation to exploring the removal efficiency of MPT it has been necessary to develop a quantitative assay (Orbell *et al.*, 1997) that can be used to compare the efficiency of MPT technology with those efficiencies offered by detergent cleansing. To this end, computer-assisted analyses such as those developed for the sequestering (Bigger *et al.*, 2010) and the sequential pick-up (Bigger *et al.*, 2013) of chemical contaminants by MPT have been used to process gravimetric laboratory data to quantitatively and objectively determine the efficiency of oil removal under a variety of conditions.

The quantitative assessment of feather condition as indicated by its coherency, on the other hand, remains an area still to be developed. It has long been recognized that feather condition, as manifested in the ability of feathers to repel water, is a key factor governing the decision as to when to release a rehabilitated bird back into the wild (Ngeh, 2002). Work on the quantitative assessment of feather condition includes early studies that applied a theory of water repellence developed by Cassie and Baxter (1944) for woven fabrics and textiles, to the structure of a feather vane (Rijke, 1968; Rijke, 1970; Rijke *et al*., 2000). It was proposed that the water repellence of contour feathers is mathematically related to the radius of the feather barb and the half-distance between the axes of the barb (Stephenson, 1997; Stephenson & Andrews, 1997).

Further to these early studies, there appears to be very little available literature on the quantitative assessment of feather condition following, say, cleansing or other rehabilitation treatments. Those that have been reported and that provide a quantitative, or at least semi-quantitative, assessment of feather condition, have been developed to varying extents. For example, the presence of preening oils in feathers has long been recognized as an important factor in enabling the feather to repel water (Elder, 1954; Stettenheim, 1972; Elowson, 1984). Based on this observation, the use of gas chromatography to quantify levels of preening oils and waxes in feathers taken from rehabilitating birds has been explored as a possible method leading to the

assessment of feather condition (Murray, 1962; Odham & Stenhagen, 1971). Other studies on the assessment of feather condition include those that report the semi-quantitative assessment of wing feather mite infestations on songbirds (Behnke *et al*., 1999; Carleton & Proctor, 2010) and the use of infrared thermography to assess laying hen feather coverage (Zhao *et al*., 2013).

A notable and more recent contribution is the work of O'Hara and Morandin (2010) who developed a barbule amalgamation index that is calculated from measurements made of feather rami taken from micrograph images. This index was used as an indicator of feather condition following exposure to oil sheens. A quantitative assessment such as this can be of significant value in the overall assessment of the condition of a bird such as a Little Penguin and, hence, in determining when to release it from a rehabilitation facility. To date, the standard international practice for deciding on the water repellency of the plumage has been to place the penguin in a pool at various stages in the rehabilitation process, monitor its behaviour and buoyancy, inspect the degree of water penetration into the plumage, and make a subjective assessment accordingly (Stocker, 2000; Department of Primary Industries, 2012). Clearly, to have a high rehabilitation success rate such practice requires a high level of experience and expertise in judging when the bird's plumage is fully water-proof and ready for release.

In view of the need for the further development of quantitative methods for the assessment of feather condition, this paper describes a computer-assisted imaging method that can be used to provide a quantitative indication of feather microstucture coherency following treatment by detergent or other cleansing actions. It is proposed that the coherence of the feather structure is an important factor that should be considered along with other factors such as the levels of preening oils and waxes when considering the water resistance and thermal insulating properties of the feather. As such, the coherence of the feather structure can be explored as an important indicator of feather condition. An indicator such as this may also have potential future use in a range of veterinary and husbandry applications.

2. Methods

2.1 Materials and Feather Characterization

Samples of breast feathers of the Mallard Duck (*Anas platyrhyhchos*) were used in this study[1]. These feathers were initially contaminated with a light crude oil (Esso, Australia, Ltd.; viscosity 11.4 cP) by immersion in the oil for 1 min. Randomly selected and uncontaminated duck feathers were used as a control. A 5% (v/v)

[1] The breast feathers of the Mallard Duck are ideal for this *proof of principle* study since they have a well-defined 2-D grid microstructure (Orbell *et al.,* 1999). It is appreciated, however, that feather microstructure is highly variable from one species to another and a specific microstructure parameter would need to be developed for each individual feather type.

cleansing detergent solution was prepared by mixing 10 mL of Decon 90™ with 190 mL of distilled water. Iron particles having an average maximum dimension of 0.21 mm were obtained from Hoganas, Sweden (grade C100.29). The particles were removed from the feathers using a "laboratory magnetic tester" supplied by Alpha Magnetics, Victoria, Australia (Orbell *et al*., 1997).

2.2 Feather Treatment and Optical Microscopy

The detergent cleansing technique involved holding a clustered sample of 5 or 6 oiled feathers by their quills (calami) and agitating in the detergent solution for a period of 10 min. The feathers were then rinsed by agitating them in distilled water for 5 min and were left to dry in air for one week. The magnetic particle cleansing treatment involved completely covering a cluster of oiled feathers with the iron particles in a Petri dish and removing all the particles with 1 to 3 continuous sweeps of the laboratory magnetic tester.

Treated single feather samples were placed on a glass plate and clamped on the stage of a Nikon optical microscope (Labophot Model 248625). Micrographs of the samples were obtained using Nikon Model 401 SLR camera fitted to the microscope.

2.3 Grid-Generating Algorithm

A Monte Carlo computer program was written to calculate the area distribution histogram of the quadrilateral elements in a randomly disrupted two-dimensional grid as a function of the extent of the imposed disruption to the grid. In the program, a square grid of side dimensions, S, comprising $n \times n$ elements was generated as a series of $n + 1$ horizontal and vertical intervals drawn between the sets of points P_1 and P_2 whose coordinates are: $P_{H,1}[x_H(i, 1), y_H(i, 1)]$; $P_{H,2}[x_H(i, 2), y_H(i, 2)]$; $P_{V,1}[x_V(i, 1), y_V(i, 1)]$ and $P_{V,2}[x_V(i, 2), y_V(i, 2)]$ and where $1 \le i \le n + 1$. The subscripts H and V represent the horizontal and vertical components respectively. The allowed deviations of the termini of each interval from their original positions on the grid is given by:

$$d = f \times S/(2n) \qquad (1)$$

where $0 < f < 1$. The parameter, f, is a constant that is set before the program is run and controls the extent of random disruption to the grid. The horizontal and vertical intervals within the perimeter of the square S are randomly disrupted by resetting the coordinates of their termini to: $P_{H,1}[0, i \times S/n + k \times d]$; $P_{H,2}[S, i \times S/n + k \times d]$; $P_{V,1}[i \times S/n + k \times d, 0)]$ and $P_{V,2}[i \times S/n + k \times d, S]$, where $2 \le i \le n$ and the constant, k, is generated randomly by the computer and lies within the limits $0 \le k \le 1$. The sign of k is also generated randomly by the computer.

A matrix of intercepts $\{x_{int}(i, j), y_{int}(i, j)\}$ is generated for the intersection of each pair of intervals for $\{(i,\ j): 2 \le (i,\ j) \le n\}$ using the following system of linear equations:

$$d_1 = x_H(i, 2) - x_H(i, 1) \tag{2}$$

$$m_1 = [y_H(i, 2) - y_H(i, 1)]/d_1, \text{ for } d_1 \neq 0 \tag{3}$$

$$d_2 = x_V(j, 2) - x_V(j, 1) \tag{4}$$

$$m_2 = [y_V(j, 2) - y_V(j, 1)]/d_2, \text{ for } d_2 \neq 0 \tag{5}$$

$$d_3 = m_2 - m_1 \tag{6}$$

$$x_{int}(i,\ j) = [m_2 x_V\ (j, 1) - m_1 x_H(i, 1) + y_H(i, 1) - y_V(j, 1)]/d_3, \text{ for } d_3 \neq 0 \tag{7}$$

$$y_{int}(i,\ j) = m_1[x_{int}(i,\ j) - x_H(i, 1)] + y_H(i, 1) \tag{8}$$

The area, A, of a quadrilateral $Q(P_1, P_2, P_3, P_4)$ defined by the points $P_1(x_1, y_1)$, $P_2(x_2, y_2)$, $P_3(x_3, y_3)$, and $P_4(x_4, y_4)$ is given by equation (9) if P_1, P_2, P_3 and P_4 lie in sequential order on the perimeter (McLanaghan & Levy, 1996):

$$A = [(x_1 y_2 - x_2 y_1) + (x_2 y_3 - x_3 y_2) + (x_3 y_4 - x_4 y_3) + (x_4 y_1 - x_1 y_4)]/2 \tag{9}$$

The area of each quadrilateral in the randomly disrupted grid is calculated systematically from the matrix of intercepts (see equations (7) and (8)) and stored in the array $A(i)$ where $1 < i < n^2$. The array $A(i)$ is then used to generate a frequency-area histogram upon multiple Monte Carlo iterations of the above algorithm.

2.4 Image Analysis Algorithm

Optical micrographs of feather images in the form of black and white photographic jpeg files were analysed using an imaging algorithm designed to systematically count white pixel areas and compile a frequency-area (count) histogram. The jpeg photographic standard stores images as a two-dimensional array of pixel information, each pixel having a red, blue and green (R, B, G) component along with "alpha" channel information associated with each pixel that determines its transparency.

The devised image processing algorithm firstly removes grey-scale shading (where R, G, B values are all equal but not equal to zero) from the image file by systematically examining the R, G, B information associated with each pixel and setting the pixel to either "white" (R = 255, G = 255, B = 255) or "black" (R = 0, G = 0, B = 0) in accordance with a (R_t, G_t, B_t) threshold set by the user. The algorithm then counts the number of sequential white pixels in each line of the image array and compiles a

histogram of the frequency of a given number of sequential white pixels. The latter is deemed to be directly related to the distribution of areas appearing within the grid pattern created by the feather microstructure.

Provision was made in the software to execute averaging cycles on the raw histogram data. In each cycle the average frequency of two successive frequencies in the histogram is calculated and recorded as the frequency of the upper of the two corresponding area ranges. This process has the effect of smoothing the distribution for the convenient analysis of the associated characteristic parameters. For the systems reported in the current work only one data averaging cycle was found to be necessary.

3. Results and Discussion

3.1 Analysis of Computer-Generated Grids

Figure 1 shows three grids that were generated by the Monte Carlo computer algorithm using three levels of grid disruption. The different extent of disruption to the coherence of the grid pattern can be clearly seen as the disruption factor, *f*, is increased from zero to 1.0.

>>>Insert Figure 1

The distribution of the individual quadrilateral areas comprising the grid as a function of the degree of disruption of the grid was explored by generating multiple grids at a given extent of disruption (*f*) and accumulating the frequencies in the area distribution histogram. The areas of the individual quadrilaterals comprising the grid were calculated in accordance with equation (9). The results are shown in Figure 2 for a selection of 20×20 grids generated with various values of the *f* parameter and where each frequency is the cumulated frequency after 100 iterations of the Monte Carlo grid disruption cycle and where a resolution of 50 area channels was used.

>>>Insert Figure 2

It is clear from Figure 2 that the width of the theoretical area distribution increases as the extent of disruption to the grid increases. There is also a noticeable shift in the maximum towards a lower value of the mean area with increasing values of *f* and possible evidence of a bimodal distribution of the quadrilateral grid areas at the extreme $f = 1$ value. The observation that there is a general broadening of the distribution with increasing *f* values supports the notion that the width of the area distribution function is an indicator of the extent of disruption to the coherence of the grid. To test the latter notion, the ratio w/h where *w* is the width of the distribution taken across the distribution at a frequency corresponding to half the maximum frequency, *h*, was plotted as a function of *f*. This plot is shown in Figure 3 for the grid

generating conditions used to create the data shown in Figure 2 and calculating data for f values ranging from 0.1 to 1.0 at increments of 0.1.

>>>Insert Figure 3

The data in Figure 3 suggest that a high degree of correlation exists between the w/h ratio and the extent of disruption to the coherence of the grid. The relationship appears to be non-linear with the sensitivity of the w/h ratio as a measure of grid coherency increasing with an increasing extent of disruption. It is also clear that the distribution of the separate areas that comprise the overall grid can, in principle, be used to measure the overall coherence of the grid pattern.

3.2 Image Analysis

3.2.1 Image Analysis of Computer-Generated Grids

Having established theoretically the relationship between the w/h ratio and the f parameter, images of the computer-generated grids were analysed using the image analysis algorithm to produce area distribution data that could be compared with those data calculated directly from the grid-generating algorithm.

Figure 4 shows a selection of area distribution plots where the data were obtained by applying the image analysis algorithm to grid images (20×20 grids; 200×200 pixels) that were, in turn, generated by the grid-generating algorithm. The histogram data were processed using one averaging cycle.

>>>Insert Figure 4

Inspection of Figure 4 reveals similar behaviour to that observed in Figure 2 and suggests that the image analysis algorithm may be used to determine area distribution data from a micrograph image and subsequently the w/h ratio for these data. To explore this further a series of images of computer-generated grids with values of the f parameter ranging from 0.1 to 1.0 at increments of 0.1 was processed using the image analysis algorithm and the w/h ratio for each grid was determined. Figure 5 shows a plot of the w/h ratio as a function of the f parameter.

>>>Insert Figure 5

Figure 5 reveals a high degree of correlation between the two variables, as was also observed in the case of Figure 3, and the relationship between the two variables is, once again, non-linear. The correspondence between the pixel areas as determined by the image analysis algorithm (i.e. a linear pixel-counting routine) and the actual areas of the grid quadrilaterals (i.e. calculated in accordance with equation (9)) can be confirmed by plotting the corresponding w/h ratios derived from each of these

techniques for the same series of computer-generated disrupted grids. Such a plot is presented in Figure 6 where $(w/h)_{\text{img anal}}$ is the w/h ratio determined from the image analysis algorithm and $(w/h)_{\text{calc}}$ is the w/h ratio determined by calculation in accordance with equation (9).

>>>Insert Figure 6

The linearity of the plot in Figure 6 confirms that the image analysis algorithm produces a reliable representation of the area distribution histogram of a disrupted two-dimensional grid and can therefore be explored further for use in determining the w/h ratio in the case of a feather micrograph image.

3.2.2 Benchmarking Image Analysis Algorithm

Previous preliminary work on feather image analysis (Ryan, 2005; Ngeh, 2002) calibrated the area distributions of feather grid patterns that were determined utilizing software that was commercially available at the time (Ryan, 2005) against distributions that were determined from a manual "cut and weigh" (CW) method. The latter involved carefully cutting out the individual grid elements from an enlarged print of the micrograph of the feather and weighing the individual pieces to indirectly determine the separate areas (Ryan, 2005). These data were then used to compile the area distribution histogram. The CW method is clearly quite tedious and can be considered somewhat subjective in that it can be difficult to treat consistently the "grey scale" regions of the image. Nonetheless, the method does provide a reasonable benchmark distribution to test the image analysis algorithm and from which to make meaningful comparisons. Furthermore, the method can overcome a difficulty that was experienced when using the commercially available area imaging software where the software did not always distinguish correctly each of the individual area components comprising the grid-like pattern. It is therefore suggested that the pixel counting algorithm described in the current work can provide a more reliable and consistent analysis of the image as it systematically counts every sequence of white pixels in the image and, as such, does not rely on the correct initial identification of the separate area boundaries.

The image analysis algorithm was further tested on the image of a feather that was previously characterized (Ryan, 2005) using the CW method described above. Figure 7 shows the area distribution histograms of the grid of a duck feather sample where the respective histograms were independently obtained using the image analysis algorithm (158 × 290-pixel micrograph) and the CW method.

>>>Insert Figure 7

To directly compare the two histograms, both the frequency and area domains were normalized with the frequency domain being normalized at the maximum frequency. Each distribution was fitted with a 6th order polynomial function to subsequently achieve a consistent analysis of its characteristic *w*/*h* parameter. Moreover, Figure 7 shows a satisfactory extent of superposition of the two distributions and further analyses of these reveals a *w*/*h* ratio calculated *via* the data obtained from the image analysis algorithm, $(w/h)_{img} = 0.962$ and that obtained *via* the CW method, $(w/h)_{CW} = 0.955$. There is only a very small difference (less than 1%) between these two values.

3.2.3 Image Analysis of Treated Feathers

Figure 8 shows micrograph images (100 × 290 pixels) of duck feather samples following treatment with detergent or magnetic particles along with the control sample (no treatment). In each case the image on the left of each pair is the original image and the image on the right of the pair is that which was obtained using the image analysis algorithm following grey scale removal. These images clearly show the extents of disruption to the grid patterns that have been imparted by the different treatments where the treatment using magnetic particles seemingly imparts less disruption to the grid pattern than that of the detergent treatment. It is important to note however, that such disruption to the grid pattern following these different treatments provides an indication of the feather condition at the time of treatment. It does not necessarily indicate the condition of the feather in the longer term when, for example, preening and the return of preening oils may improve feather condition.

>>>Insert Figure 8

The images shown in Figure 8 were further analysed using the software and the respective area distribution histograms were produced (see Figure 9). The plots in Figure 9 confirm quantitatively the observations that can be made by visual inspection of Figure 8. The profiles of the control sample and the sample treated with magnetic particles are similar and have *w*/*h* ratios of 0.561 and 0.600 respectively. This represents a difference of *ca*. 7%. The *w*/*h* ratio for the detergent-treated sample is significantly greater (0.743) than either of the latter (difference of *ca*. 20%).

>>>Insert Figure 9

The distribution histogram for the detergent treated sample exhibits a long "tail" that corresponds to the larger open areas in its grid-like pattern. These are apparent in the corresponding micrograph image and reflect the greater extent of disruption to the grid pattern caused by the detergent treatment as compared with the magnetic particle treatment (see Figure 8). A very strong correlation between the *w*/*h* ratio for feathers treated with detergent and the concentration of detergent has also been shown to exist

(Orbell *et al*., 2007) in the case where the *w*/*h* ratio was determined manually using the CW method.

4. Conclusions

The image analysis algorithm developed in this work provides a reliable quantitative means of determining the coherency of a two-dimensional grid-like pattern that reflects the feather microstructure of the Mallard Duck. The algorithm produces a result that is consistent with theoretical computer-generated grids as well as with the pattern observed in the micrographs of the feather microstructure. This analysis technique successfully identified differences in the grid coherency of the feather structure following different cleansing treatments and, as such, is proposed as a possible quantitative indicator of the condition of this type of feather at the point in time following the treatment. The effects of residual oil, metal, detergent or other contaminants on the outcome produced by the technique has not been taken into account and is yet to be explored.

Nonetheless, this work provides an important proof of principle, namely that such indicators could be useful for the routine quantitative assessment of feather condition, either for the trialling of different treatment protocols, as a tool during the rehabilitation process, or as an assessment of feather condition in veterinary studies along with other indicators, to give a more complete and objective assessment of feather condition than is currently possible. Furthermore, it is suggested that the method will be a valuable tool in helping to answer some remaining key questions such as: how much if any, of the feather disruption is permanent and how much can be reversed by preening and what is the impact of this disruption on a whole living animal and its feathers in a variety of different environments and life stages. Work along these lines is continuing in our laboratory.

Acknowledgements

This work was conducted with the support of the Australian Research Council under ARC Linkage Grant #LP0989407. The authors are also grateful to the Phillip Island Nature Parks, the Penguin Foundation and Google for their generous support of this work.

References

Behnke, J., McGregor, P., Cameron, J., Hartley, I., Shepherd, M., Gilbert, F., Barnard, C., Hurst, J., Gray, S., Wiles, R., 1999. Semi-quantitative assessment of wing feather mite (*Acarina*) infestations on passerine birds from Portugal. Journal of Zoology, 248(3), 337-347.

Bigger, S.W., Ngeh, L.N., Orbell, J.D., 2010. Mathematical model for the sequestering of chemical contaminants by magnetic particles. Journal of Environmental Engineering, 136(11), 1255-1259.

Bigger, S.W., Munaweera, K., Ngeh, L.N., Dann, P., Orbell, J.D., 2013. Mathematical model for the sequential pick-up of chemical contaminants by magnetic particles. Journal of Environmental Engineering, 139(6), 796-802.

Carleton, R.E., Proctor, H.C., 2010. Feather mites associated with eastern bluebirds (*Sialia sialis L.*) in Georgia, including the description of a new species of *Trouessartia* (*Analgoidea: Trouessartiidae*). Southeastern Naturalist, 9(3), 605-623.

Cassie, A.B.D., Baxter, S., 1944. Wettability of porous surfaces. Transactions of the Faraday Society, 40**,** 546-541.

Department of Primary Industries (2012). Procedure – Oil/Chemical Spill Wildlife Response – Rehabilitation of Wildlife. Biosecurity Operations Branch. Orange, New South Wales, Australia. 12 pp. [Available at: http://www.dpi.nsw.gov.au/__data/assets/pdf_file/0008/432098/Oil-Chemical-Spill-Wildlife-Response-Rehabilitation-of-Wildlife-V1.pdf]

Elder, W.H., 1954. The oil glands of birds, The Wilson Bulletin, 66, 6-31.

Elowson, A.M., 1984. Spread-wing postures and the water repellency of feathers: A test of Rijke's hypothesis, The Auk, 101(2), 371-383.

McLanaghan, K., Levy, S., 1996. CRC Standard Mathematical Tables and Formulae (D. Zwillinger, Ed.) 30th edn., CRC Press, Boca Raton, Ch. 4, p. 270.

Murray, K.E., 1962. Studies in waxes. Australian Journal of Chemistry, 15(3), 510-520.

Ngeh, L.N., 2002. The development of magnetic particle technology for application to environmental remediation. PhD Thesis, Victoria University, Australia, Ch. 5.

Ngeh, L.N., Orbell, J.D., Bigger, S.W., Munaweera, K., Dann, P., 2012. Magnetic cleansing for the provision of a 'quick clean' to oiled wildlife. World Academy of Science, Engineering & Technology, 72, 1091-1093.

Odham, G., Stenhagen, E., 1971. On the chemistry of preen gland waxes of waterfowl. Accounts of Chemical Research, 4(4), 121-128.

O'Hara, P.D., Morandin, L.A., 2010. Effects of sheens associated with offshore oil and gas development on the feather microstructure of pelagic seabirds. Marine Pollution Bulletin, 60, 672-678.

Orbell, J.D., Godhino, L., Bigger, S.W., Nguyen, T.M., Ngeh, L.N., 1997. Oil spill remediation using magnetic particles – An experiment in environmental technology. Journal of Chemical Education, 74(12), 1446-1448.

Orbell, J.D., Ngeh, L.N., Bigger, S.W., Zabinskas, M., Zheng, M., Healy, M., Jessop, R., Dann, P., 2004. Whole-bird models for the magnetic cleansing of oiled feathers. Marine Pollution Bulletin, 48(3), 336-340.

Orbell, J.D., Dao, H.V., Ngeh, L.N., Bigger, S.W., 2007. Magnetic particle technology in environmental remediation and wildlife rehabilitation. Environmentalist, 27, 175-192.

Rijke, A.M., 1968. The water repellency and feather structure of cormorants, *Phalacrocoracidae*. Journal of Experimental Biology, 48(1), 185-189.

Rijke, A.M., 1970. Wettability and phylogenetic development of feather structure in water birds. Journal of Experimental Biology, 52(2), 469-479.

Rijke, A.M., Jesser, W.A., Evans, S.W., Bouwman, H., 2000. Water repellency and feather structure of the blue swallow *Hirundo atrocaerulea*. Ostrich, 71(1-2), 143-145.

Ryan., S., 2005. The development of a quantitative indicator of feather damage utilizing digital imaging technology. MSc Thesis, Victoria University, Australia, Ch. 5.

Safarikova, M., Safarik, I., 2001. The application of magnetic techniques in biosciences. Magnetic and electrical Separation, 10(4), 223–252.

Stephenson, R., 1997. Effects of oil and other surface-active organic pollutants on aquatic birds. Environmental Conservation, 24(2), 121-129.

Stephenson, R., Andrews, C.A., 1997. The effect of water surface tension on feather wettability in aquatic birds. Canadian Journal of Zoology, 75(2), 288-294.

Stettenheim, P.R., 1972. The Integument of Birds. In: Farmer, D.S., King, J.R. (Eds.) Avian Biology. Academic Press, New York, Vol. 2, pp. 1-63.

Stocker, L., 2000. Practical Wildlife Care, Blackwell Science, London.

Zhao, Y., Yin, H., Dong, B., 2013. Use of infrared thermography to assess laying hen feather coverage. Poultry Science, 92(2), 295-302.

514 **Figure Captions**
515
516 **Fig 1**. Two-dimensional grids generated by the Monte Carlo computer algorithm and
517 that were randomly disrupted using disruption factors of: (i) $f = 0$, (ii) $f = 0.6$
518 and (iii) $f = 1.0$.
519
520 **Fig 2**. Selection of area distribution histograms for the quadrilaterals comprising
521 computer-generated 20 × 20 grids subjected to different extents of random
522 disruption as determined by the disruption parameter f where: $f = 0.3$ (filled
523 circles), $f = 0.6$ (open circles) and $f = 0.9$ (filled squares).
524
525 **Fig 3**. Plot of the ratio w/h *versus* the disruption parameter f for a computer-
526 generated grid where the grid component areas were calculated from equation
527 (9). Calculation parameters: 20 × 20 grid; 100 iterations; 50 channels area
528 resolution.
529
530 **Fig 4**. Selection of area distribution histograms for 20 × 20 grids produced by the
531 grid generating algorithm and where the images were processed by the image
532 analysis algorithm using 1 data averaging cycle. Disruption parameters: $f =$
533 0.3 (filled circles), $f = 0.6$ (open circles) and $f = 0.9$ (filled squares).
534
535 **Fig 5**. Plot of the ratio w/h *versus* the disruption parameter f for area distribution
536 histogram data derived from computer-generated 20 × 20 grids where the
537 images were processed by the image analysis algorithm using 1 data averaging
538 cycle.
539
540 **Fig 6**. Plot of $(w/h)_{\text{img anal}}$ *versus* $(w/h)_{\text{calc}}$ where the corresponding ratios were
541 determined for a series of computer-generated grids with the disruption
542 parameter f varying between 0.1 and 1.0 at increments of 0.1.
543
544 **Fig 7**. Area distribution histograms of the grid-like pattern of a Mallard Duck feather
545 micrograph where the distributions were independently determined using: (i)
546 the image analysis algorithm (filled circles) and (ii) the CW method (open
547 circles).
548
549 **Fig 8**. Micrograph images (5×) of Mallard Duck feather samples following treatment
550 with: (i) detergent and (ii) magnetic particles. The control sample (no
551 treatment) is also shown. In each pair of images, the image on the left is the
552 original and the one on the right is the corresponding image with its grey scale
553 removed.
554
555

Fig 9. Area distribution histograms derived from the image analysis algorithm (5 data averaging cycles) for Mallard Duck feather samples (Figure 8) that were subjected to: (i) detergent (filled squares) and (ii) magnetic particle (open circles) treatment. The control sample (filled circles) is shown for comparison.

Figure 1

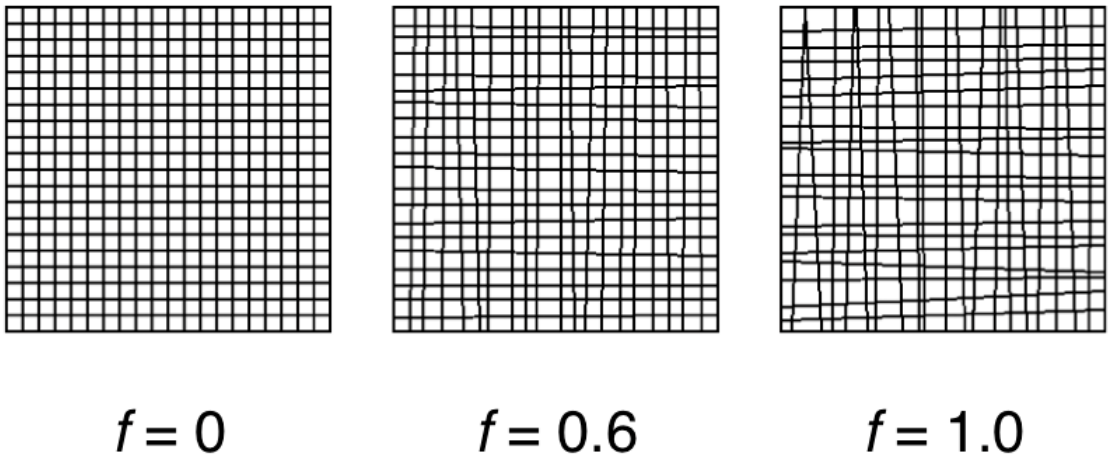

Figure 2

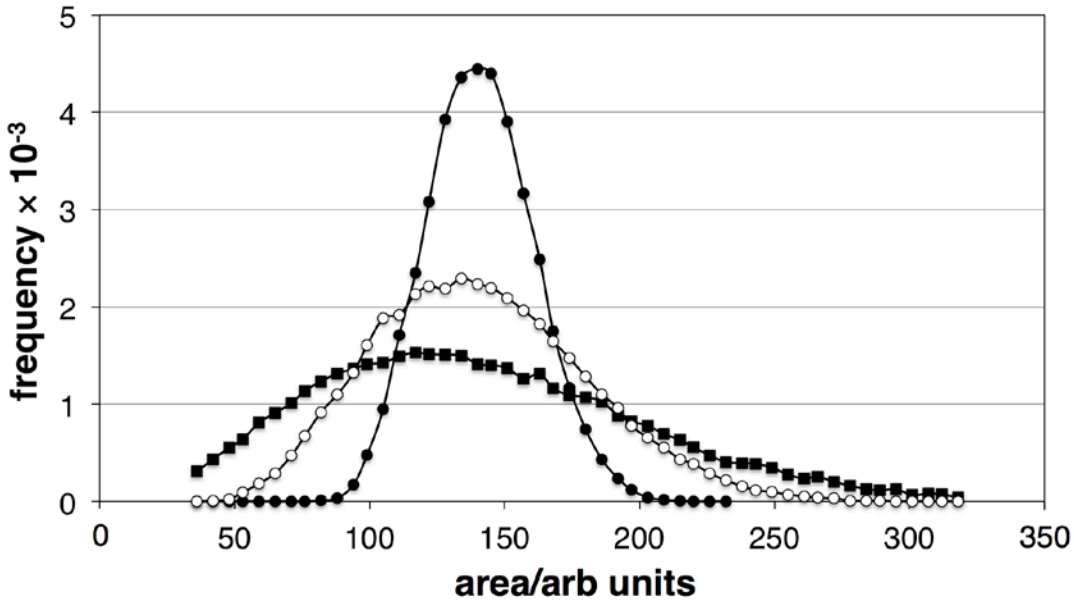

Figure 3

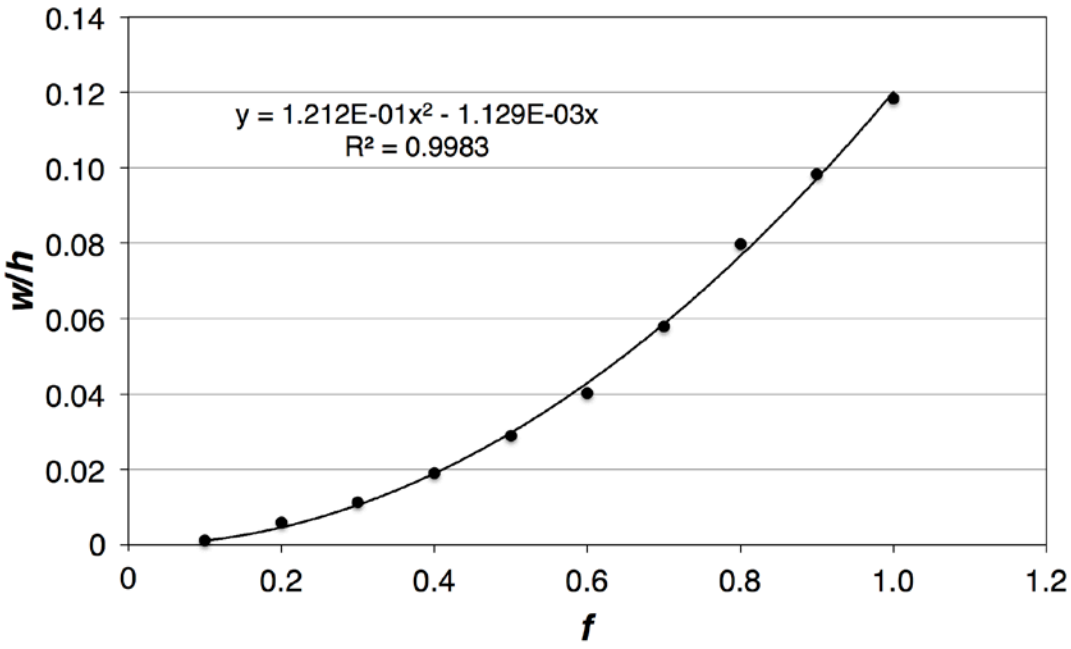

Figure 4

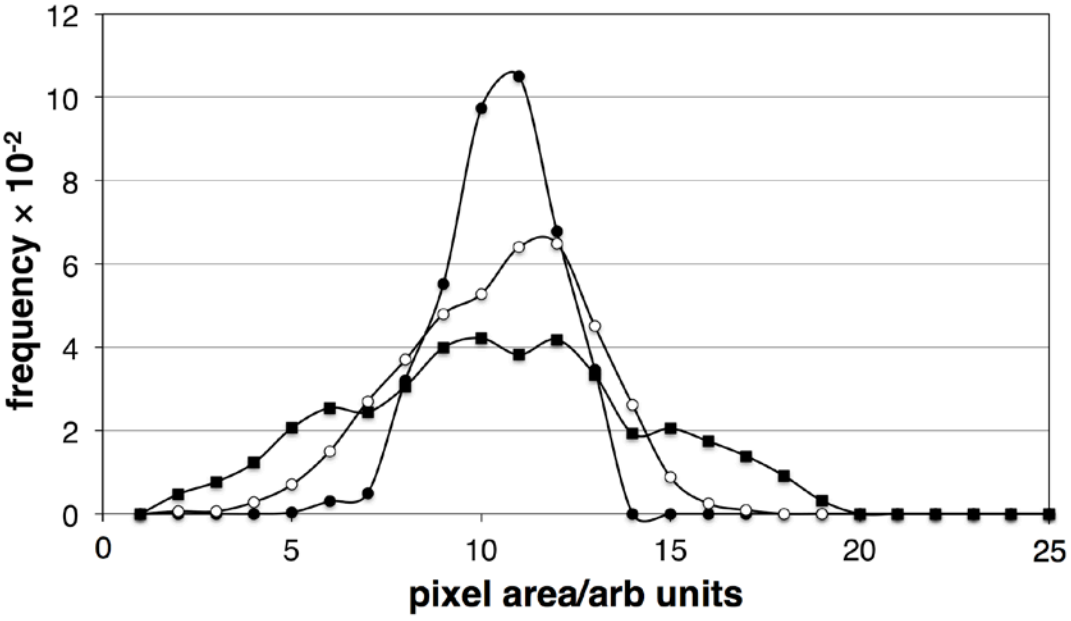

Figure 5

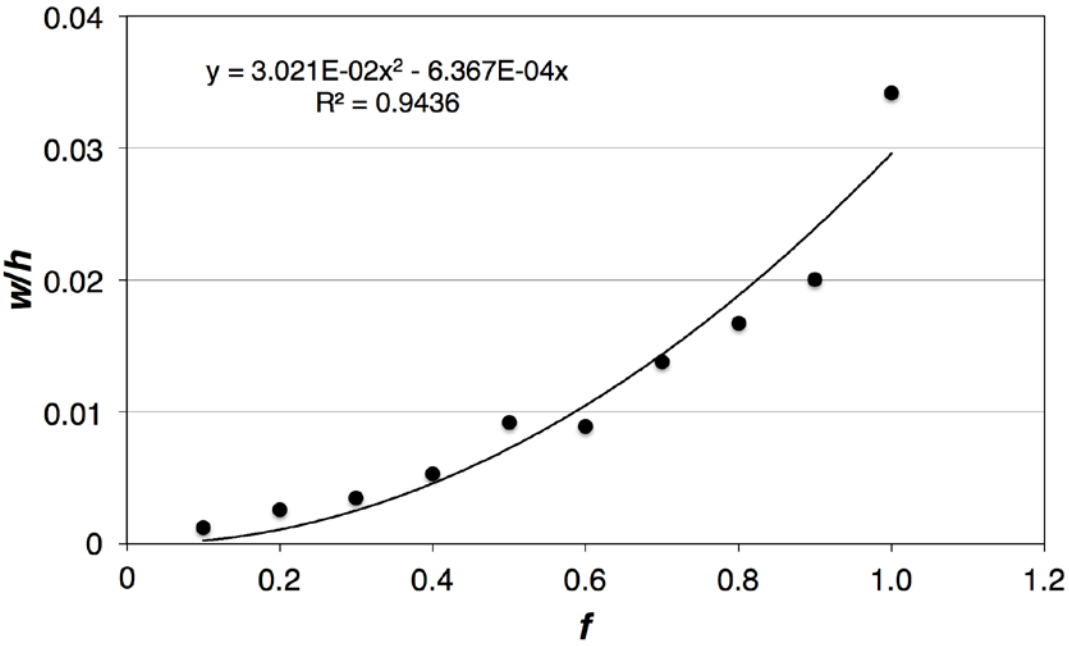

Figure 6

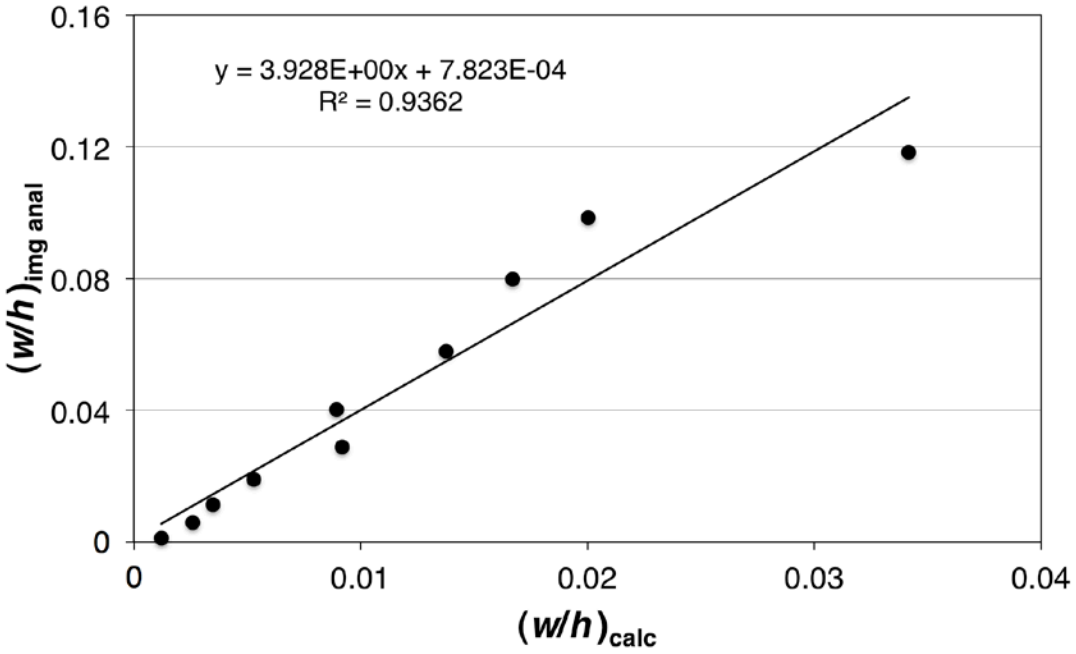

Figure 7

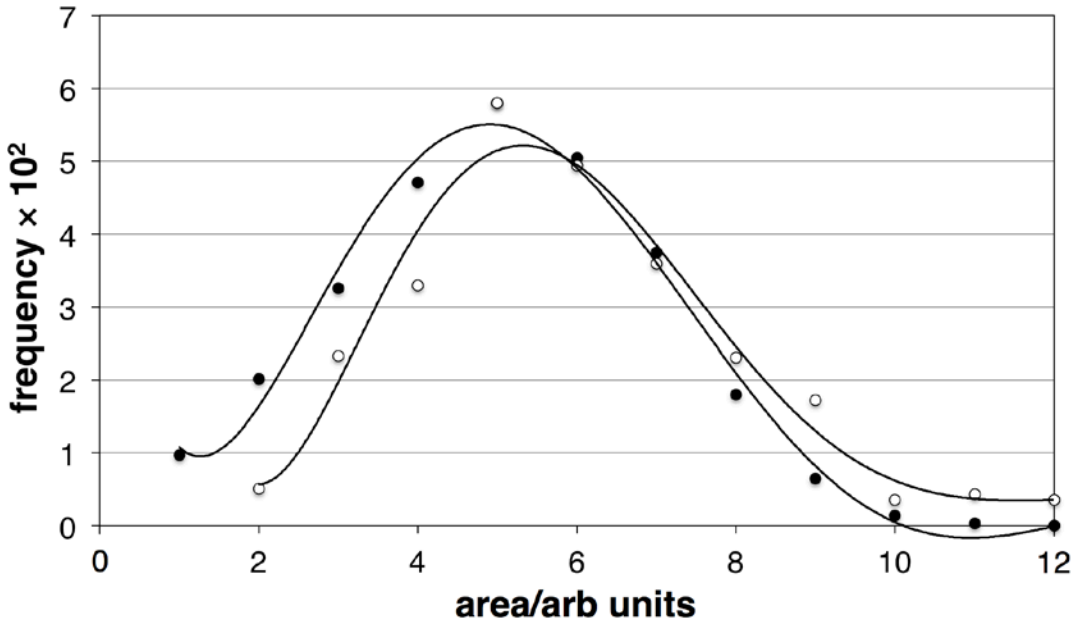

Figure 8

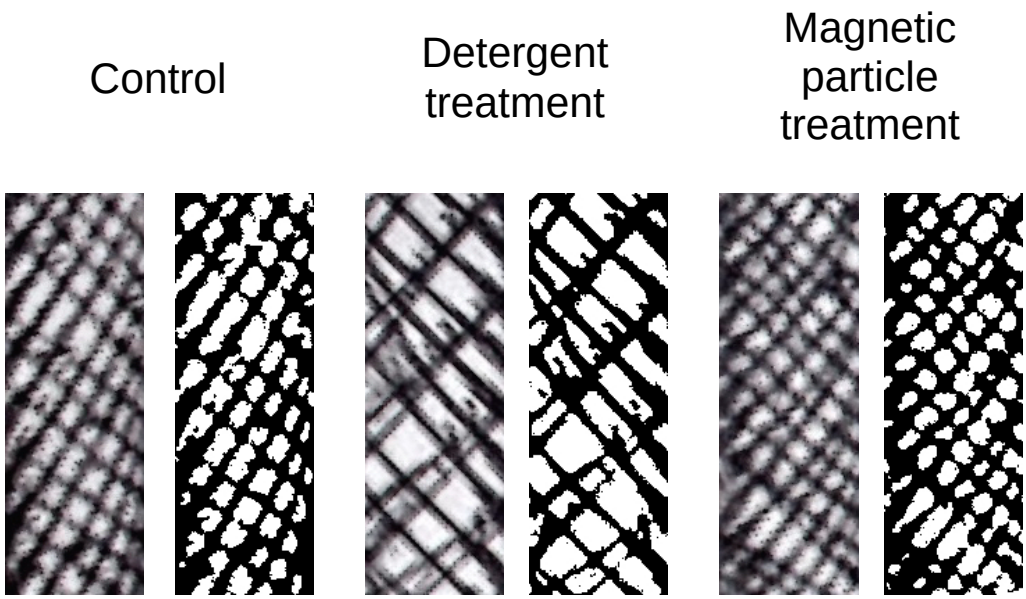

733 **Figure 9**
734
735

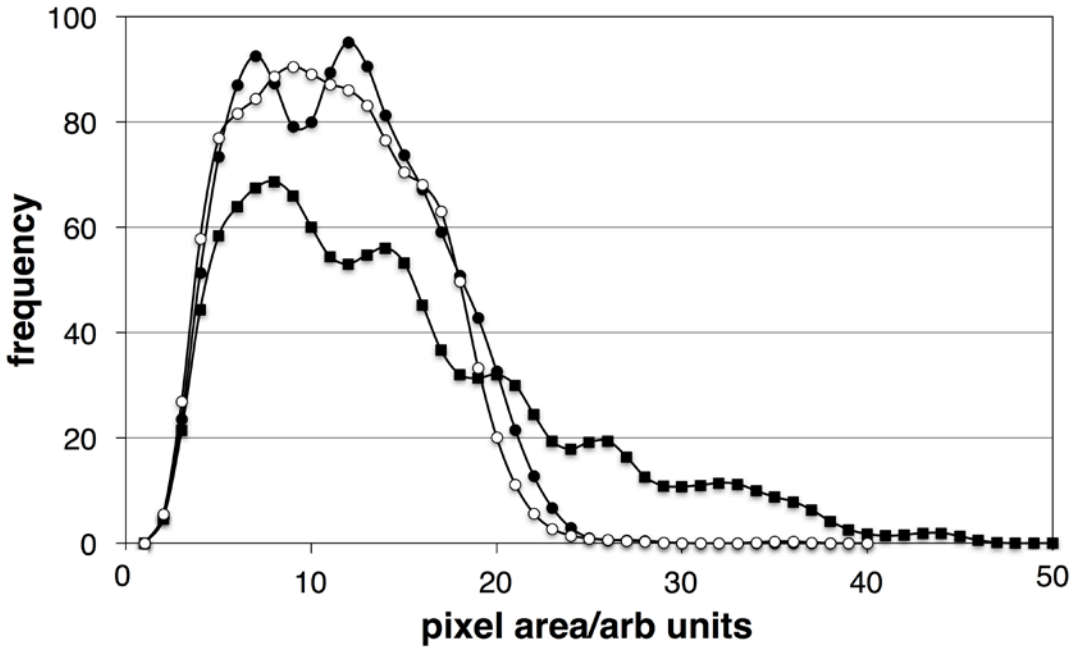

736
737
738
739
740
741